http://dx.doi.org/10.5012/bkcs.2012.33.8.2699

Modified Equation for Predicting the Radius of Assembled Superstructures Made of Nanowires Including Polypyrrole Segment of All Length Scales

Jong Kuk Lim

Department of Chemistry, Chosun University, Gwangju 501-759, Korea. E-mail: jklim@chosun.ac.kr
Received March 6, 2012, Accepted May 18, 2012

Gold-polypyrrole segment nanowires prepared using anodized aluminum oxide templates can be assembled into a curved superstructure that shows stimuli-induced contraction and expansion. The radius of the superstructures can be predicted using the simple equation suggested by J. K. Lim *et al*. (*Nano Lett.* 8, 4441 (2008)). The suggested equation, however, is valid only within the limiting condition in that the length of the polypyrrole segment is comparable to, or much longer than the gold segment. In this study, the original equation was modified to a new equation that is valid for all length scales of polypyrrole segments. The radius of the superstructures calculated using the modified equation was compared with the result calculated by the original equation, and the validity of the modified equation is discussed.

Key Words : Self-assembly, Segment nanowire, Actuation, Polypyrrole, Stimuli

Introduction

Gold (Au)-polypyrrole (PPy) segment nanowires prepared using anodized aluminum oxide (AAO) templates can be assembled into a curved superstructure. The orientation of the nanowires is determined by the AAO templates, and the nanowires are collected by the capillary force of water. The volume of the PPy segment decreases with the evaporation of water from the matrix of the PPy segments. The difference in diameter between the Au and PPy segments is affected by the volume of PPy, and the assembled nanowires are rolled up to form a curved superstructure (Figure 1(a)).[1-3]

Recently, it was reported that external stimuli, such as humidity, temperature and light, can induce actuation of the assembled superstructures.[4] The suggested mechanism is that the actuation of superstructures is driven by a change in volume of the PPy segment, which resulted from the re-evaporation or re-absorption of water in the PPy segment. At low humidity, or high temperatures, the volume of the PPy segment is decreased by the re-evaporation of water from the matrix of the PPy segment. On the other hand, water is re-absorbed to the matrix of the PPy segment in high humidity, or at low temperatures.[5] Light dependence of the superstructures can be explained using the same mechanism as the photothermal effect because PPy absorbs light at all wavelengths, and photothermal conversion occurs efficiently in PPy.[6]

The radius of superstructures can be predicted by the simple equation suggested by J. K. Lim *et al*.[4] The suggested equation, however, is valid only under limiting conditions. The equation is based on the assumption that the length of the PPy segment is comparable to, or much longer than the gold segment resulting in two almost parallel adjacent nanowires, or a very small angle, α, between the adjacent PPy segments (Figure 1). In this study, the original equation was modified to a new equation, which is available for a short PPy segment, or large angle, α, as well as a long PPy segment, or small angle, α.

Modification of the Original Equation

Figure 1 shows the definitions of "R_o", "R_i", "l_{Au}", "l_{PPy}", "C_i" , and "α". The outer radius of the superstructures, R_o, is the sum of the inner radius, R_i, and the length of Au segment,

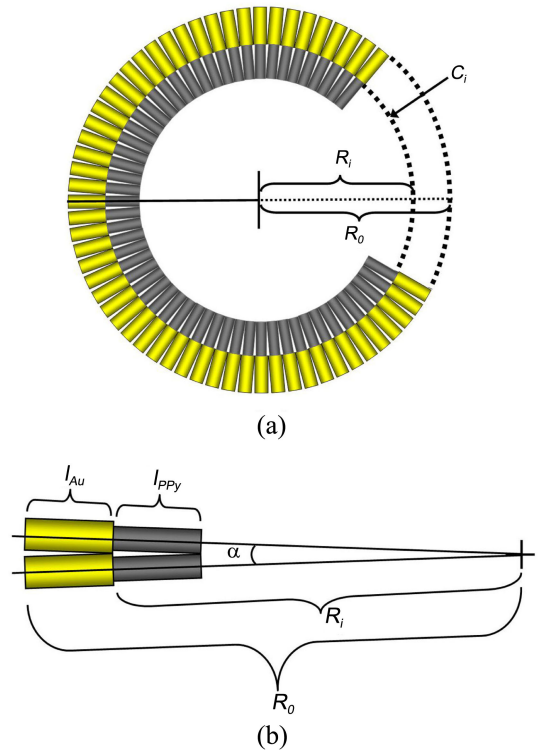

Figure 1. Schematic diagram of the curved superstructures composed of Au-PPy segment nanowires through the guidance of AAO templates, (a), and its magnified image, (b).

l_{Au} (Eq. (1)).

$$R_o = R_i + l_{Au} \tag{1}$$

The inner radius, R_i is calculated from the hypothetical circumference of the inner circle, C_i, of the superstructures. In the original equation, C_i is obtained by multiplying the number of nanowires, N, needed to form a complete circle with the diameter of the Au segment, d_{Au} (Eq. (2)).[4]

$$C_i(=2\pi R_i) \approx N \cdot d_{Au} \tag{2}$$

where

$$N = \frac{2\pi}{\alpha} = \frac{2\pi}{2\tan^{-1}(\Delta d/2l_{PPy})} \tag{3}$$

In Eq. (3), "Δd" is defined as the difference in diameter between the Au and PPy segments, which is $\Delta d = d_{Au} - d_{PPy}$.

The predicted C_i calculated by Eq. (2) is the circumference represented by the length of the black bold line in Figure 2(a). The length of the black bold line closely approaches the real C_i, as α decreases, or the length of PPy, l_{PPy} increases. On the other hand, the predicted C_i calculated using Eq. (2) will deviate from the real C_i if α becomes large, or l_{PPy} becomes much smaller than l_{Au}. This is a reasonable result because, in Eq. (2), the number of nanowires, N, is multiplied by d_{Au}, which is constant for α. Consequently, the difference in radius between the predicted C_i and real C_i increases with increasing α, or with decreasing l_{PPy}. To better predict the real C_i, the length of the dashed line should be calculated as a circumference instead of the length of the black bold line in Figure 2(a).

The part of the dashed line from "A" to "B" in Figure 2(a) is defined as "s" in Figure 2(b), which is a close up of the part of the region in Figure 2(a). The length of the dashed line from "A" to "B" is related to Δd and α (Eq. (4)).

$$\frac{s}{2} = \frac{\Delta d}{2}\cos\left(\frac{\alpha}{2}\right)$$

$$\therefore\ s = \Delta d \cos\left(\frac{\alpha}{2}\right) \tag{4}$$

Finally, modified Eq. (5) can be derived from original Eq. (2). In Eq. (5), d_{Au} is replaced with the sum of d_{PPy} and "s".

$$C_i(=2\pi R_i) \approx N \cdot \left(d_{PPy} + \Delta d \cos\left(\frac{\alpha}{2}\right)\right) \tag{5}$$

The modified equation was used to describe the assembled superstructures made from short or long PPy segments.

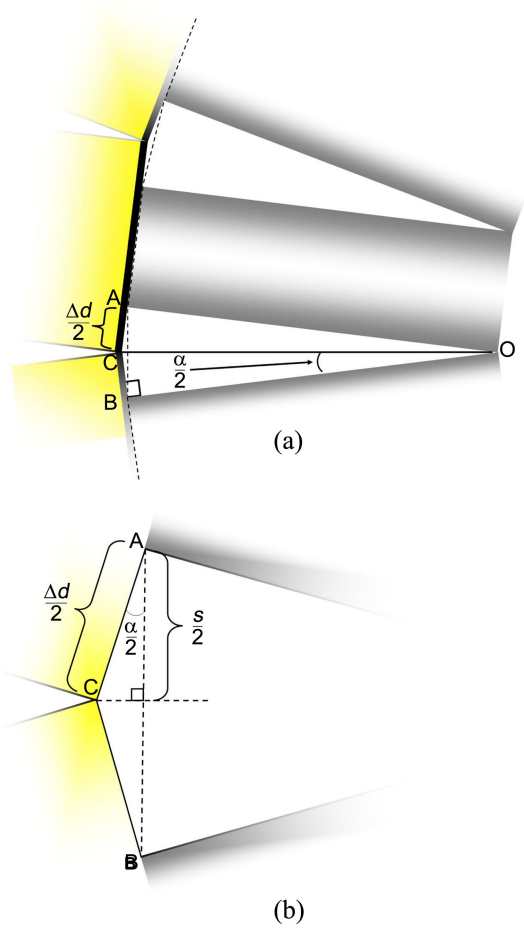

Figure 2. The original equation was modified to estimate the circumference represented by the dashed line instead of the black bold line, (a). From the geometry shown in (b), "s" can be related to "Δd and "α".

Results and Discussion

In Eq. (2), it was assumed that α is very small. This assumption is reasonable when the length of the PPy segment is long (l_{PPy} > ~1 μm), or the adjacent nanowires are almost parallel. In this length (l_{PPy} > ~1 μm), the value of α is almost "zero", and does not vary with the length of the PPy segment and Δd, as shown in Figure 3. On the other hand, as the length of the PPy segment is short (l_{PPy} < ~1 μm) α becomes large (Figure 3) and strongly dependent on Δd (the inset of Figure 3). Hence, the assumption of a small

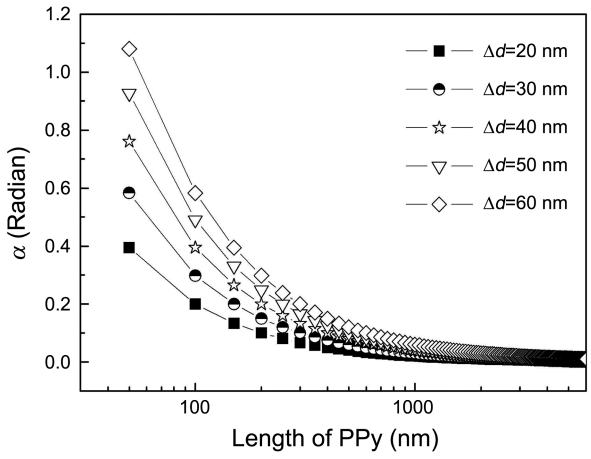

Figure 3. The angle, α, varies with the length of PPy, l_{PPy} and Δd. The value of α increases slowly with decreasing l_{PPy} from 6 μm to ~1 μm, and increases rapidly as l_{PPy} decreases below ~1 μm. The superstructures made from short PPy (l_{PPy} < ~1 μm) have a different α according to Δd.

α for Eq. (2) is not acceptable in the case of a short PPy segment. This incorrect assumption results in an error in the predicted radius of the superstructures comprising of short PPy segments. Eq. (5), however, is available in all length scales of the PPy segment because "$d_{PPy} + s$" in Figure 2(b) is used in Eq. (5) instead of "d_{Au}". In Eq. (2), "d_{Au}" is constantly independent of "α", but "s" in Eq. (5) is a function of "α", which varies with the change in l_{PPy}.

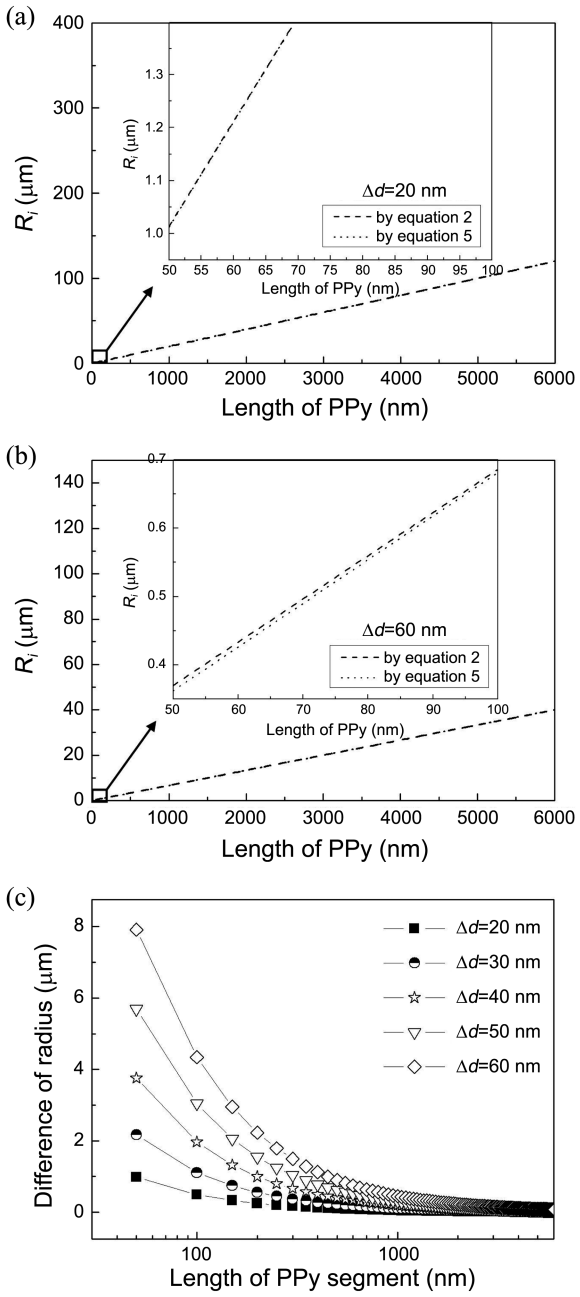

Figure 4. The estimated inner radius of the superstructures at Δd = 20 nm calculated using Eq. (2) is in accordance with the radius by Eq. (5), (a). At Δd = 60 nm, however, the difference between the estimated inner radii of the superstructures calculated by Eq. (2) and (5) diverges with decreasing PPy length (b). Difference in the radius (R_i calculated using Eq. (2) – R_i calculated by Eq. (5)) was plotted as a function of the length of PPy, (c). The difference in radius is large in a short PPy, at large Δd.

The inner radius of the superstructure, R_i, was calculated using Eqs. (2) or (5), and compared with each other at different Δd (Figure 4(a), (b)). In both cases, R_i decreased with decreasing l_{PPy}. At a small Δd (= 20 nm), R_i calculated using Eq. (2) was varied in accordance with R_i calculated using Eq. (5) (the inset of Figure 4(a)). On the other hand, at large Δd (= 60 nm), R_i calculated using Eq. (2) deviates from R_i calculated by Eq. (5) with decreasing l_{PPy}. The difference in the radius of the superstructures (R_i calculated using Eq. (2) – R_i calculated using Eq. (5) was plotted as a function of l_{PPy} (Figure 4(c)). In Figure 4(c), the difference in the radius of the superstructures was almost "zero" at a long PPy segment (l_{PPy} > ~1 μm), but the difference in the radius of the superstructures becomes large as the length of the PPy segment is short (l_{PPy} < ~1 μm) (the inset in Figure 4(c)). The inner radius of the superstructures, R_i, which was calculated using Eq. (5) decreased with increasing α, because α is a function of the cosine in Eq. (5). In addition α increased when l_{PPy} was short (Figure 3). Consequently, R_i varies consistently with l_{PPy}. On the other hand, R_i calculated using Eq. (2) did not change with α. Therefore, the difference in the radius of the superstructures (R_i calculated by Eq. (2) – R_i calculated by Eq. (5)) diverges with decreasing l_{PPy}. In addition, the difference in the radius of the superstructures became large when Δd was increased from 20 to 60 nm.

In a previous paper, the outer radius of the superstructure was predicted to be ~77.6 μm using Eq. (2) based on the assumption that nanowires contain Au and PPy segments, 3.4 and 8.9 μm in length and 400 and 352 nm in diameter, respectively.[4] The same paper reported that the opening and closing of the assembled superstructures can be activated by several external stimuli, such as humidity, temperature and light. In high humidity, at low temperatures, or under irradiation of intense light, the radii of the superstructures contracted, and it was predicted that the radius of the superstructures shrank by ~80% of their original values (defined as "contraction ratio"), when the diameter and length of the PPy segment had decreased by ~11 nm (from 352 to 341

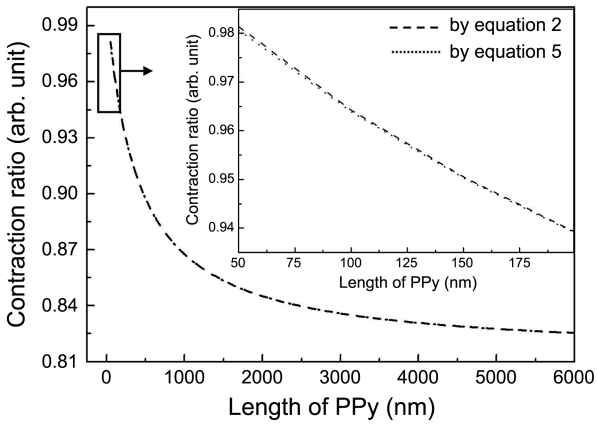

Figure 5. The contraction ratios defined as the ratio of the radii of the superstructures before and after contraction were calculated using Eqs. (2) or (5) at different lengths of the PPy segment, and plotted as a function of the PPy segment length. Two curves are almost the same at all PPy segment lengths (inset).

nm) and ~0.3 μm (from 8.9 to 8.6 μm), respectively.

This contraction ratio varies with the length of the PPy segment, l_{PPy} (Figure 5). When l_{PPy} was decreased from 6 μm to 50 nm, the contraction ratio increased from ~83% to ~98% (Figure 5). The contraction ratios were calculated using either Eqs. (2) or (5), and plotted as a function of l_{PPy} to compare the variance of the contraction ratios with each other. Unlike the difference in radius (Figure 4(c)), both contraction ratios were similar (the inset of Figure 5), even in a short PPy segment.

Conclusion

An equation for predicting the radius of the assembled superstructures and their contraction ratios was introduced in a previous study. Since that equation was based on the assumption of a long PPy segment, it was expected that the predicted radius and contraction ratio using the same equation would deviate from the real values for a superstructure made from a short PPy segment. Herein, a more general equation was newly induced to better describe the assembled superstructures and the results from both equations (original and modified equations) were compared. The difference in radii predicted from both equations increased with decreasing length of the PPy segment. The difference in radii increased more rapidly at a large Δd than at a small Δd, but the contraction ratios predicted from both equations were similar at all length scales.

Acknowledgments. This study was supported by research funds from Chosun University, 2011. The author wishes to acknowledge Ms. Jihee Jo and Mr. Byoung Gue Jung for their help.

References

1. Park, S.; Lim, J.-H.; Chung, S.-W.; Mirkin, C. A. *Science* **2004**, *303*, 348.
2. Ciszek, J. W.; Huang, L.; Wang, Y.; Mirkin, C. A. *Small* **2008**, *4*, 206.
3. Ciszek, J. W.; Huang, L.; Tsonchev, S.; Wang, Y.; Shull, K. R.; Ratner, M. A.; Schatz, G. C.; Mirkin, C. A. *ACS Nano* **2010**, *4*, 259.
4. Lim, J. K.; Ciszek, J. W.; Huo, F.; Jang, J.-W.; Hwang, S.; Mirkin, C. A. *Nano Lett.* **2008**, *8*, 4441.
5. Okuzaki, H.; Funasaka, K. *Synth. Met.* **2000**, *108*, 127.
6. Huang, J.; Kaner, R. B. *Nature Mater.* **2004**, *3*, 783.